Biological Journal of the Linnean Society, 2018, **XX**, 1–17. With 5 figures.

Molecular and morphometric analyses reveal cryptic diversity within freshwater mussels (Bivalvia: Unionidae) of the western Gulf coastal drainages of the USA

ANNA M. PIERI[1], KENTARO INOUE[1]*, NATHAN A. JOHNSON[2], CHASE H. SMITH[2,3], JOHN L. HARRIS[4], CLINT ROBERTSON[5] and CHARLES R. RANDKLEV[1]

[1]*Natural Resources Institute, Texas A&M University, Dallas, TX 75252, USA*
[2]*US Geological Survey, Wetland and Aquatic Research Center, Gainesville, FL 32653, USA*
[3]*Biology Department, Baylor University, Waco, TX 76798, USA*
[4]*Department of Biological Sciences, Arkansas State University, Jonesboro, AR 72467, USA*
[5]*Texas Parks and Wildlife Department, River Studies Program, San Marcos, TX 78667, USA*

Received 12 February 2018; revised 29 March 2018; accepted for publication 29 March 2018

Past geological processes and climate change affected current species distributions and the genetic structure of riverine fauna. Western Gulf of Mexico coastal rivers harbour four mussel species within the genus *Fusconaia* (Bivalvia: Unionida). The distributions of these species are unclear owing to their indistinguishable shell morphologies. Using molecular phylogenetic and Fourier morphometric analyses, we examined phylogenetic relationships and morphological variation among the species and made inferences about the role of past geological and climatic factors in shaping the current genetic structure and distributions of these species in the region. Our results showed the presence of three *Fusconaia* species within the region: *Fusconaia askewi*, *Fusconaia chunii* and *Fusconaia flava*. We confirmed that *Fusconaia lananensis* is a junior synonym of *F. askewi* and that *F. chunii* is genetically distinct from *F. askewi*. The Trinity River has syntopic *F. flava* whose morphologies are indistinguishable from those of *F. chunii*. Divergence-time estimates matched major geological and climatic events in the region, where climate-driven river formations during the mid-Miocene to Pleistocene caused major diversification of *Fusconaia* species. Knowledge gained from the present study provides a better understanding of vicariant events that shaped current species distributions and helps to identify conservation priorities that apply to the *Fusconaia* species.

ADDITIONAL KEYWORDS: allopatric speciation – conservation priorities – divergence time – Fourier shape morphometrics – fluvial morphology – molecular clock – riverine ecosystems – vicariance.

INTRODUCTION

Geological processes and climate change play important roles in promoting speciation of aquatic organisms (Near & Benard, 2004; Berendzen *et al.*, 2007). In riverine systems, the dominant mode of speciation stems from vicariant events followed by allopatric speciation (Mayden, 1988; Near & Benard, 2004; Thesing *et al.*, 2016). Changes in river courses, which tend to fragment populations, are driven by interacting tectonic uplift and long-term climatic factors (Galloway, Whiteaker & Ganey-Curry, 2011; Hoagstrom *et al.*, 2013). For example, drastic climate fluctuations, such as the Pleistocene glacial cycles, altered watercourses by rerouting rivers and depositing sediments in alluvial plains (Mayden, 1988; Strange & Burr, 1997). Such processes drive geographical isolation, which in turn restricts gene flow between fragmented populations, after which genetic drift and local adaptation facilitate further population divergence until eventually lineages become reproductively incompatible. Given human-driven climate change and anthropogenic disturbance of habitats, it is important to understand evolutionary responses to vicariant events and to develop effective conservation practices for taxa in peril.

Rivers in the western Gulf of Mexico coastal plain of the USA and Mexico have been shaped by climate change and by geological events such as the landscape evolution of the Mississippi River valley,

*Corresponding author. E-mail: kentaro.inoue@ag.tamu.edu

formation of the Rocky Mountains, thermally driven uplift, volcanism, and sea-level change in the Gulf of Mexico (Galloway *et al.*, 2011). These events have resulted in a series of isolated river systems on the Gulf coastal plain that vary in size, geomorphology and hydrology. In turn, this isolation, coupled with varying environmental conditions, has led to high levels of endemism across these drainages (Neck, 1982; Haag, 2010; Howells, 2010; Tockner, Lorang & Stanford, 2010; Burkhead, 2012). Although the western Gulf coastal drainages exhibit relatively low richness of freshwater fish species compared with the Interior and Appalachian highlands of North America (Mayden, 1992), they have high levels of endemism and disproportionate numbers of extinct species of freshwater fishes (Burr & Mayden, 1992; Burkhead, 2012). This is also true for other freshwater taxa in the region, such as freshwater mussels (Neck, 1982; Howells, Neck & Murray, 1996; Haag, 2010; Howells, 2010).

Freshwater mussels (Bivalvia: Unionida) inhabit all continents (except Antarctica) and reach their highest diversity in North America (Graf & Cummings, 2007; Bogan & Roe, 2008; Graf, 2013). Currently, four major faunal regions are recognized based on the biogeographical patterns of freshwater mussels, namely the Mississippian, Eastern Gulf, Atlantic and Pacific regions (Haag, 2010, 2012). Of ~300 currently recognized taxa (Williams *et al.*, 2017), two-thirds of the mussel species are found in the Mississippian Region, which includes the entire Mississippi River basin, the Great Lakes system, and all Gulf of Mexico river systems from the Mobile River basin west to the Rio Grande basin (Haag, 2010). Although the mussel assemblages among basins within the Mississippian Region are similar, there is some level of endemism, which varies across basins. For example, in the Sabine–Trinity Province, which includes the Calcasieu, Neches, Sabine and Trinity River systems in eastern Texas and western Louisiana (Neck, 1982; Haag, 2010), four nominal species in the genus *Fusconaia* have been recognized: *Fusconaia askewi* (Marsh, 1896), *Fusconaia chunii* (Lea, 1862), *Fusconaia flava* (Rafinesque, 1820) and *Fusconaia lananensis* (Frierson, 1901). *Fusconaia askewi* presumably occurs in all rivers in the Sabine–Trinity Province in addition to the Sulphur River and Big Cypress Bayou of the Red River drainage (Neck, 1982; Howells *et al.*, 1996). *Fusconaia chunii* is endemic to the Trinity River and often is considered a junior synonym of *F. flava* (Vidrine, 1993; Howells *et al.*, 1996; Haag, 2010). *Fusconaia flava* is widely distributed in the Mississippian Region from western New York to eastern Kansas and from the Great Lakes system to the Gulf of Mexico coastal drainages (Watters, Hoggarth & Stansbery, 2009). *Fusconaia lananensis* is thought to be endemic to the Angelina River, some of its tributaries, and possibly Village Creek within the Neches River basin (Howells *et al.*, 1996).

Recent molecular analyses of this group drew the following conclusions: (1) *F. askewi* may not occur in the Calcasieu River (Burlakova *et al.*, 2012); (2) *F. lananensis* is not a valid species and is likely to be a junior synonym of *F. askewi* (Burlakova *et al.*, 2012; Campbell & Lydeard, 2012a); (3) *F. chunii* is likely to be a senior synonym of *F. askewi* (Burlakova *et al.*, 2012); and (4) *F. flava* is likely to occur in parts of the Sabine–Trinity and Mississippi Embayment provinces of Louisiana (i.e. the Calcasieu River and Red River drainages; Burdick & White, 2007; Burlakova *et al.*, 2012). Based on these findings, Williams *et al.* (2017) recognized *F. chunii* as a senior synonym of *F. askewi* and *F. lananensis*. However, the previous molecular and taxonomic studies did not assess *F. chunii* from the type locality (Trinity River, Dallas, TX), *F. lananensis* from the type locality (Lanana Creek, a tributary of the Neches River) or *Fusconaia* sp. from Big Cypress Bayou, San Jacinto River, Sulphur River and Trinity River. Furthermore, a more recent phylogenetic study of the tribe Pleurobemini (which includes the genus *Fusconaia*) indicated that *F. chunii* from the Trinity River is genetically distinct from *F. askewi* or *F. flava* (Inoue *et al.*, 2018).

In this study, we used molecular phylogenetic and Fourier shape morphometric analyses to resolve questions regarding the evolutionary history and taxonomic status of four *Fusconaia* species thought to occur in the Sabine–Trinity Province. The objectives were as follows: (1) to delineate species boundaries within the four *Fusconaia* species by testing phylogenetic relationships and estimating divergence time among species using two mitochondrial DNA (mtDNA) genes and one nuclear DNA (nDNA) fragment; (2) to quantify morphological variation among species using Fourier shape analysis; and (3) to infer the roles of past geological and climatic factors in shaping the current genetic structure and distributions of these species within the province. Currently, *F. askewi* and *F. lananensis* are listed as threatened in the state of Texas (TPWD, 2010), and *F. lananensis* has been proposed for listing under the US Endangered Species Act (ESA) by the US Fish and Wildlife Service (USFWS, 2009). Therefore, our findings are crucial to the state and federal agencies that need defensible taxonomic and biogeographical information to develop conservation strategies for these species.

MATERIAL AND METHODS

We collected 131 individuals of *F. askewi* from the Neches and Sabine River drainages, 74 individuals of *F. chunii* from the Trinity River drainage (including

the San Jacinto River) and 83 individuals of *F. flava* from six major river drainages in Arkansas, Louisiana and Texas (including the Big Cypress Bayou and Sulphur River) for molecular and morphometric analyses (Supporting Information, Table S1; Fig. 1). Additionally, for genetic analyses, we obtained a dried tissue sample from a paratype specimen of *F. lananensis* (Lanana Creek; Baylor University Mayborn Museum Collection: MO33569) and collected *Fusconaia burkei* (Ortmann & Walker, 1922) from the Choctawachee River drainage, *Fusconaia cerina* (Conrad, 1838) from the Pascagoula and Tombigbee River drainages [type locality: waters of Louisiana, not far from New Orleans (Conrad, 1838)]; *Fusconaia escambia* Clench & Turner, 1956 from the Escambia River drainage, *Fusconaia masoni* (Conrad, 1834) from the Neuce and Tar River drainages, *Fusconaia mitchelli* (Dall, 1896) from the Guadalupe River, and *Pleurobema riddellii* (Lea, 1862) from the Neches and Sabine River drainages.

Initial species identifications of the collected samples were made based upon the collection locality and shell morphology. Given that *F. askewi* and *F. lananensis* were difficult to distinguish based on their shell morphologies, we assigned all individuals from the Neches and Sabine rivers to *F. askewi*, except for published sequences from GenBank and the paratype specimen of *F. lananensis* from Lanana Creek. Live specimens were euthanized with 95% ethanol and then separated into soft tissue and shell. Soft tissue was preserved in 95% ethanol until DNA extraction, and shells used for morphometric analyses were scrubbed inside and out to remove any remaining tissue. Detailed locality and voucher information for the collected specimens is provided in the Supporting Information (Table S1). Our samples included individuals at or near the type locality of the target species: *F. askewi* from Village Creek, TX (a tributary of the Neches River); *F. cerina* from Twelvemile Creek,

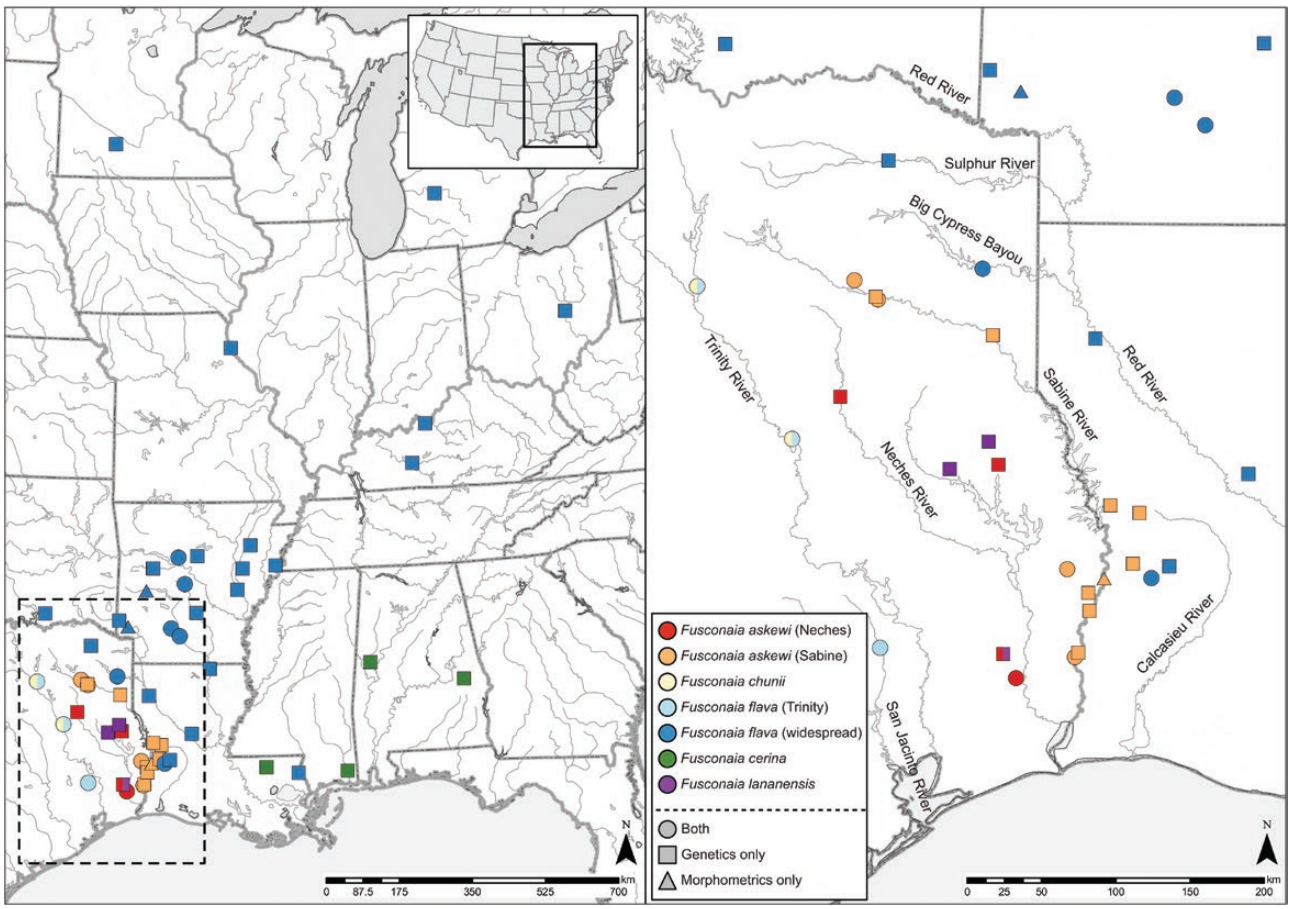

Figure 1. Collection localities for specimens of target species used in this study. Colours represent target species and collected drainages (red, *Fusconaia askewi* from the Neches River; orange, *F. askewi* from the Sabine River; yellow, *Fusconaia chunii* from the Trinity River; light blue, *Fusconaia flava* from the Trinity and San Jacinto rivers; blue, widespread *F. flava*; green, *Fusconaia cerina*; purple, *Fusconaia lananensis*). Shapes correspond to specimens used for genetics only (squares), morphometrics only (triangles) or for both genetic and morphometric analyses (circles).

LA (a tributary of Lake Pontchartrain); *F. chunii* from the Trinity River near Dallas, TX; *F. flava* from the Green River, KY (a tributary of the Ohio River); and *F. lananensis* from Lanana Creek, TX (a tributary of the Neches River) (Supporting Information, Table S1; Fig. 1). For further genetic comparison, we obtained previously published sequences for *F. askewi*, *F. cerina*, *F. chunii*, *F. flava* and *F. lananensis* from GenBank (Supporting Information, Table S1).

We extracted genomic DNA from mantle tissue using standard cetyltrimethylammonium bromide (CTAB)/chloroform extraction followed by ethanol precipitation (Saghai-Maroof *et al.*, 1984). We amplified two mtDNA genes, cytochrome *c* oxidase subunit I (*cox1*) and NADH dehydrogenase subunit 1 (*nad1*), and one nDNA segment, internal transcribed spacer 1 (ITS1). We used the *cox1* primers described by Folmer *et al.* (1994), the *nad1* primers described by Campbell *et al.* (2005) and the ITS1 primers described by King *et al.* (1999). We followed the recommended thermal conditions for polymerase chain reaction (PCR) provided in the original literature. Owing to the difficulty in amplifying *cox1*, we used two alternative *cox1* primer sets described by Campbell *et al.* (2005) and Inoue, Lang & Berg (2015). The PCR products were visualized using 1% agarose gel electrophoresis and purified with ExoSAP-IT (Affymetrix) or GenCatch Gel Extraction Kit (Epoch Life Science). We employed Eurofins Genomics (Louisville, KY) for DNA sequencing. Sequences were assembled and aligned using SeqMan Pro v14.0 (DNASTAR, Madison, WI, USA), and an open-reading frame for the two mtDNA genes was verified. Ambiguous sequences of both the 3′ and the 5′ end were trimmed. We used MAFFT v7 (Katoh & Standley, 2013) to perform multiple sequence alignment.

We generated TCS haplotype networks (Clement, Posada & Crandall, 2000) for *cox1*, *nad1* and ITS1 separately in POPART (http://popart.otago.ac.nz/). We colour-coded each haplotype by species and drainage of collection. Phylogenetic trees were reconstructed using Bayesian inference (BI) and maximum likelihood (ML) based on three datasets: concatenated mtDNA (i.e. *cox1* and *nad1*; hereafter, mtDNA dataset), ITS1 dataset, and concatenated mtDNA and nDNA (i.e. *cox1*, *nad1* and ITS1; hereafter, mtDNA + nDNA dataset). Note that because of the limited number of ITS1 sequences, we reduced numbers of *cox1* and *nad1* sequences to match the number of ITS1 sequences for the mtDNA + nDNA dataset. We included 17 species in the tribe Pleurobemini [13 *Fusconaia* species, three *Pleurobema* species and *Eurynia dilatata* (Rafinesque, 1820); Supporting Information, Table S1] to evaluate phylogenetic relationships. We also included *Arcidens confragosus* (Say, 1829), *Cyclonaias petrina* (Gould, 1855) and *Quadrula apiculata* (Say, 1829) as outgroups. Before the phylogenetic analyses, we used METAPIGA v3.1 (Helaers & Milinkovitch, 2010) to identify unique haplotypes and evaluate substitution saturation for each dataset. We only used unique haplotypes for the phylogenetic analysis and used KAKUSAN4 (Tanabe, 2011) to estimate the best-fit model of nucleotide substitution for each codon partition of *cox1* and *nad1*. Based on Bayesian information criterion (BIC), the best substitution model for the *cox1* dataset was GTR + Γ for the first codon, F81 for the second codon and HKY + Γ for the third codon. For the *nad1* dataset, the best substitution model was K80 + Γ for the first codon and HKY + Γ for the second and third codons. The best substitution model for ITS1 dataset was K80 + Γ.

Phylogenetic analyses were performed with MrBayes v3.2.6 (Ronquist *et al.*, 2012) and RAxML v8.2.10 (Stamatakis, 2014). In MrBayes, two simultaneous Markov Chain Monte Carlo (MCMC) runs (each chain containing three heated chains and one cold chain) were executed for 8×10^6 generations, with trees sampled every 1000 generations for a total of 8001 trees in the initial sample. We used Tracer v1.5 (Rambaut & Drummond, 2009) to assess the convergence of both MCMC runs by plotting the log-likelihood scores for each sampled point. When the likelihood values reached a plateau with sufficient effective sample sizes (ESS > 200), we considered the Markov chains stationary. Accordingly, we discarded the first 25% of trees (2000 trees) as burn-in, and the remaining trees were retained and evaluated using the 50% majority rule for a consensus tree. For the ML analysis, we set GTR + Γ for all gene and codon partitions and used 1000 rapid bootstraps to calculate nodal support values.

We used DnaSP v5.10 (Librado & Rozas, 2009) to estimate the number of haplotypes (H), mean number of nucleotide differences (K) and mean nucleotide diversity (π) from each gene for seven groups. The groups were assigned to individuals by species identified by the phylogeny and collected drainages (i.e. *F. askewi* from the Neches River, *F. askewi* from the Sabine River, *F. cerina* from the eastern Gulf of Mexico coastal drainages, *F. chunii* from the Trinity River, *F. flava* from the Trinity River, *F. flava* from elsewhere, and *F. lananensis* from the Neches River). We used MEGA v7.0.16 (Kumar, Stecher & Tamura, 2016) to estimate pairwise genetic divergence (uncorrected p-distance) between groups separately for the mtDNA and ITS1 datasets.

We used a molecular clock method implemented in BEAST v2.4.5 (Bouckaert *et al.*, 2014) to estimate divergence time among *Fusconaia* species, with a focus on *Fusconaia* species within the Sabine–Trinity Province. We used the mtDNA + nDNA dataset and all *Fusconaia* species (i.e. 13 species), and included

Pleurobema clava (Lamarck, 1819) as the outgroup. A random starting tree was estimated under the HKY + Γ model for all loci with estimated base frequencies. A relaxed lognormal clock model and coalescent-constant-population model were used. We used two *cox1* substitution rates available for Unionida (Bolotov *et al.*, 2016; Froufe *et al.*, 2016). These included *cox1* substitution rates of $2.56 \times 10^{-9} \pm 0.6 \times 10^{-9}$ substitutions per site year^{-1} estimated from two *Unio* species currently separated by the Strait of Gibraltar (Froufe *et al.*, 2016) and substitution rates of 1.68×10^{-9} to 2.86×10^{-9} substitutions per site year^{-1} estimated from fossil records of *Margaritifera* species (Bolotov *et al.*, 2016). Analysis was run for 5×10^7 generations, with sampling every 1000 generations and a burn-in of 25% of the total saved trees, and the remaining trees were retained and evaluated using the maximum clade credibility method for a consensus tree.

We used two generalized mixed Yule-coalescent (GMYC) methods, the Bayesian GMYC model (bGMYC; Reid & Carstens, 2012) and the single-threshold GMYC model (ST-GMYC; Pons *et al.*, 2006), to delimit putative species for *Fusconaia*. Briefly, the GMYC model identifies boundaries between branching events that are either divergent between species (Yule process) or diversification within species (coalescence) under the assumption that speciation processes occur at a lower rate than population processes (Fujita *et al.*, 2012). We used ultrametric trees generated by BEAST analyses based on the mtDNA + nDNA dataset. We used the 'splits' package (Ezard, Fujisawa & Barraclough, 2013) in R to conduct ST-GMYC analysis on the consensus tree using the single-threshold method and default intervals. For the bGMYC analysis, we randomly selected 100 ultrametric trees from the 37 500 trees after burn-in from BEAST. With the 'bGMYC' package (Reid & Carstens, 2012) in R, we ran 100 000 MCMC generations, sampled the state every 100 generations, and discarded 3000 trees as burn-in. We set the threshold parameter priors, t1 and t2, to 2 and 100, respectively, and the starting parameter value was set at 40. We used a single point estimate approach to delimit species boundaries; thus, we used the bgmyc.point function to set the delimitation threshold relative to the posterior mean of the analysis at 0.5.

We used Fourier shape morphometrics to compare the outlines of shell shapes among populations and species. We used *F. askewi* collected from the Neches and Sabine rivers, *F. chunii* from the Trinity River, and *F. flava* from the Trinity River. Additionally, we included *F. flava* collected from the Arkansas River drainage (West Fork Point Remove Creek, AR), Calcasieu River drainage (Bundick Creek, LA), Ouachita River drainage (the mainstem, Little Missouri River, and North Fork of the Saline River, AR) and Red River drainage (Cossatot River, AR) (Supporting Information, Table S2; Fig. 1). We tested five groups: *F. askewi* (Neches), *F. askewi* (Sabine), *F. chunii* (Trinity), *F. flava* (Trinity) and *F. flava* (widespread). We took digital photographs of the right valve of each specimen with a Canon EOS7D SLR camera. We first extracted the outline of the shell by cropping the image using Adobe Photoshop CC v2015.0.0 (Adobe Systems). Using cropped shell images, the shell outline was described by 20 Fourier coefficients using SHAPE v1.3 (Iwata & Ukai, 2002). We analysed morphological variation within and between groups through principal component analysis (PCA) and used multivariate analysis of variance (MANOVA) and discriminant function analysis (DFA) to determine how frequently principal component (PC) scores correctly distinguished between groups. We created a confusion matrix based on the DFA, where we calculated proportions of correct group assignments by the DFA. We used the first ten PC axes for MANOVA and DFA.

RESULTS

We examined ~658 bp of the *cox1* gene from 270 individuals, ~608 bp of the *nad1* gene from 163 individuals, and ~533 bp of the ITS1 spacer region from 105 individuals (Supporting Information, Table S1). New sequences obtained for this study were submitted to GenBank (accession numbers: MH133466–MH133899; Supporting Information, Table S1). We did not find any indication of substitution saturation in the datasets.

Haplotype networks revealed two distinct clusters in the *cox1* and *nad1* datasets (Fig. 2A, B), whereas there was no genetic structure among species in the ITS1 dataset (Fig. 2C). In both mtDNA networks, one cluster was composed of *F. askewi* from the Neches and Sabine rivers, *F. chunii* from the mainstem of the Trinity River above Lake Livingston and the East Fork of the Trinity River, and *F. lananensis* from the Neches River. The other cluster consisted of *F. cerina* from the eastern Gulf of Mexico coastal drainages, individuals initially identified as *F. chunii* from the East Fork of the San Jacinto River and the mainstem of the Trinity River (hereafter, *F. flava* from the Trinity River), and *F. flava* collected from elsewhere (hereafter, widespread *F. flava*). For the first cluster, *F. askewi* shared the same haplotypes between drainages and exhibited a relatively high number of haplotypes (15 and 17 for *cox1* and *nad1*, respectively). Those haplotypes were shared with *F. lananensis* in both *cox1* and *nad1* networks. *Fusconaia chunii* had unique haplotypes distinct from those of *F. askewi* and *F. lananensis*. In the second cluster, *F. flava* from the Trinity River shared the same haplotype with widespread *F. flava* in the *cox1* network

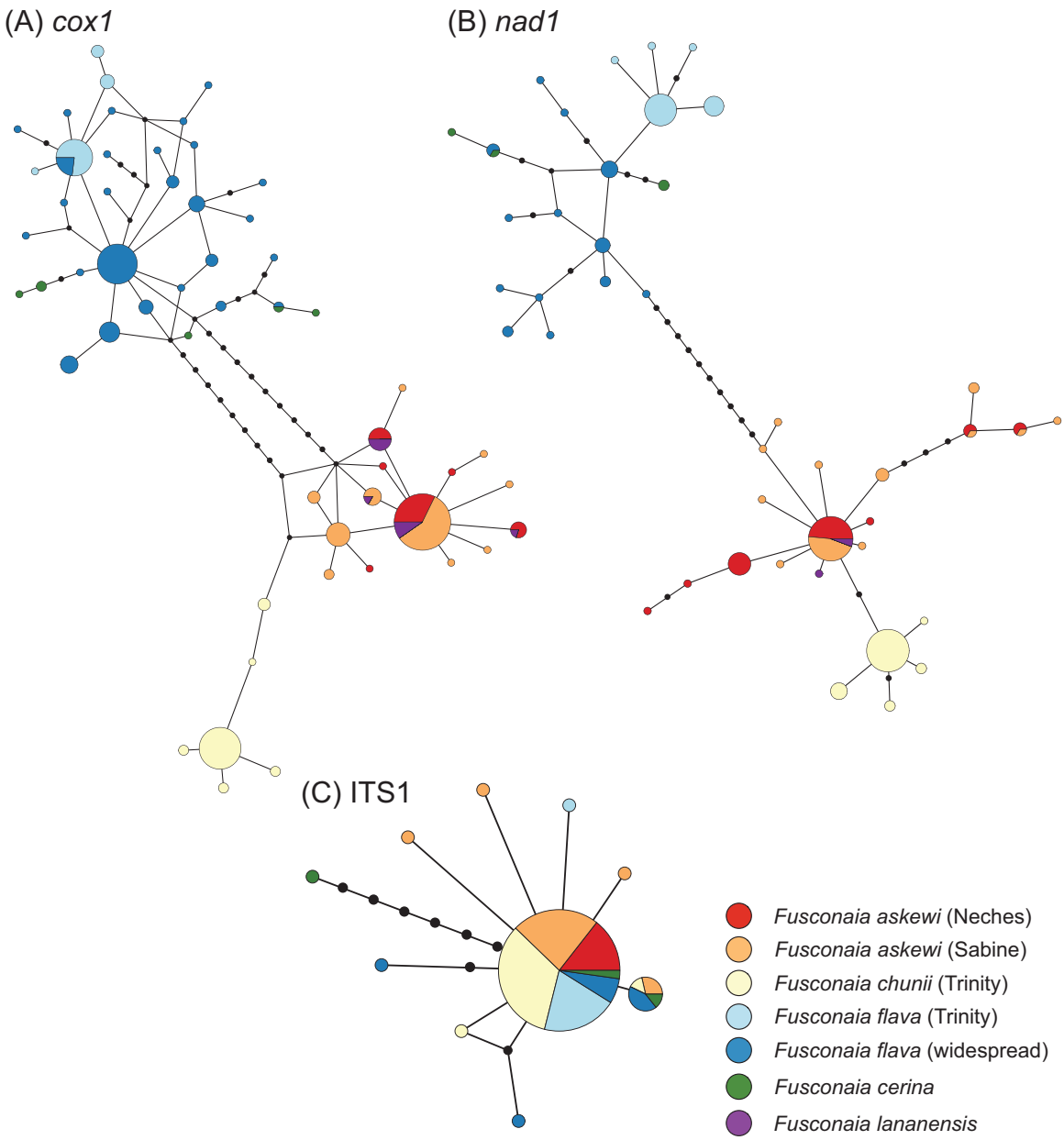

Figure 2. Haplotype networks of *Fusconaia* species for *cox1* (A), *nad1* (B) and ITS1 (C). Colours correspond to species and collected drainages (red, *Fusconaia askewi* from the Neches River; orange, *F. askewi* from the Sabine River; yellow, *F. chunii* from the Trinity River; light blue, *Fusconaia flava* from the Trinity River; blue, widespread *F. flava*; green, *Fusconaia cerina*; purple, *Fusconaia lananensis*). Note that no ITS1 genotype was sequenced for *F. lananensis*. Each line represents one base-pair difference between haplotypes, black dots are inferred missing haplotypes, and haplotype frequency is relative to the size of the circles.

(Fig. 2A), whereas *F. flava* from the Trinity River had unique haplotypes in the *nad1* network (Fig. 2B). In the *cox1* and *nad1* networks, *F. cerina* shared the same haplotype with widespread *F. flava*. For the ITS1 network, all four species (*F. askewi*, *F. cerina, F. chunii* and *F. flava*, including ones from the Trinity River and elsewhere) shared a single haplotype (Fig. 2C).

The BI and ML phylogenies showed similar tree topologies and nodal supports. The phylogenies based on the mtDNA and mtDNA + nDNA datasets showed similar tree topologies and a monophyletic clade for the genus *Fusconaia* with high nodal supports (Fig. 3; Supporting Information, Fig. S1). Within *Fusconaia*, species generally formed monophyletic clades with

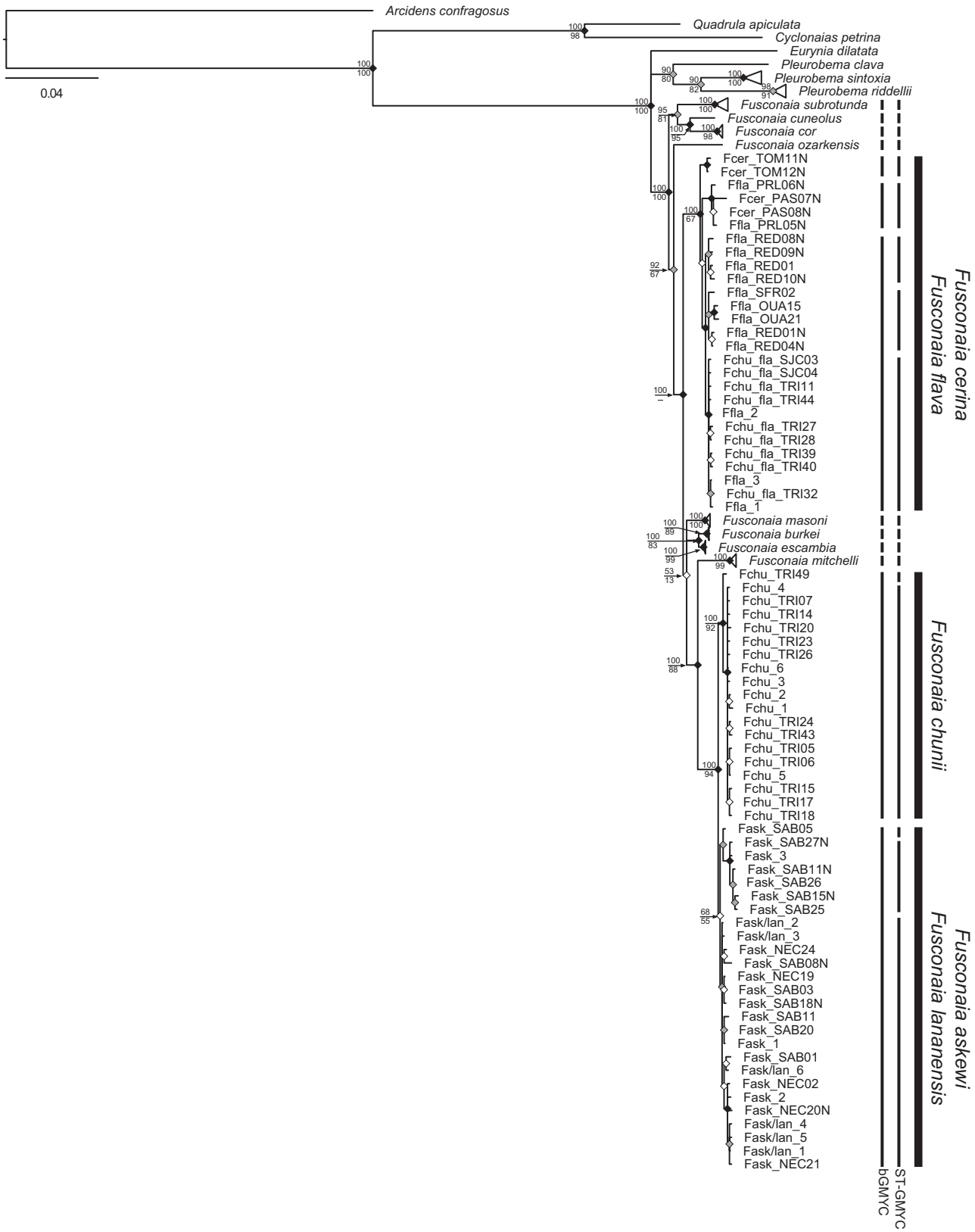

Figure 3. Phylogenetic tree reconstructed by Bayesian analysis for concatenated mitochodrial DNA and nuclear DNA (i.e. *cox1*, *nad1* and ITS1) sequence dataset. Values above branches represent Bayesian posterior probabilities and values below

high nodal supports. *Fusconaia chunii* formed a monophyletic clade, which is sister to a monophyletic clade of *F. askewi* and *F. lananensis* with shallow branch separation, and no *F. chunii* individuals placed in the *F. askewi*/*F. lananensis* clade. Like the *cox1* and *nad1* haplotype networks, *F. askewi* and *F. lananensis* shared the same clade and did not show geographical structure between drainages. *Fusconaia chunii* had high nodal support, whereas the *F. askewi*/*F. lananensis* clade had low support. The clade of *F. askewi*/*F. lananensis* and *F. chunii* formed a sister clade with *F. mitchelli* with a high nodal support. *Fusconaia flava* did not show geographical structure, and *F. cerina* formed paraphyletic clades, which clustered within the *F. flava* clade (Fig. 3; Supporting Information, Fig. S1). *Fusconaia cerina* from the Pascagoula River shared a clade with *F. flava* from the Pearl River. The phylogenies based on the ITS1 dataset showed no resolution within Pleurobemini (i.e. *Eurynia*, *Fusconaia* and *Pleurobema*; Supporting Information, Fig. S2). One haplotype was shared among *F. cerina*, *F. chunii*, *F. flava* and *F. askewi*.

For mtDNA genes, genetic diversity was similar among groups except for widespread *F. flava* (Table 1). The number of haplotypes within groups ranged from four to ten for *F. askewi*, *F. cerina*, *F. chunii*, *F. flava* from the Trinity River, and *F. lananensis*. Widespread *F. flava* had high genetic diversity (i.e. number of haplotypes and mean nucleotide diversity). For ITS1, genetic diversity was similarly low among groups except for *F. cerina* (Table 1). The number of haplotypes ranged from one to five, and mean nucleotide diversity ranged from zero to 0.0103 for ITS1. For the mtDNA dataset, pairwise genetic divergence among species ranged from 0.0096 (*F. askewi* from the Neches River vs. *F. chunii*) to 0.0386 (*F. chunii* from the Trinity River vs. *F. flava*; Table 2). For the ITS1 dataset, genetic divergence among populations and species was relatively low (range 0.0001–0.0061; Table 2).

Time-calibrated phylogenies generated from BEAST analyses were generally congruent with the BI phylogeny based on the mtDNA + nDNA dataset (Fig. 4); however, the BEAST tree resolved polytomic clades where the clade of *F. burkei* and *F. escambia* formed sister to the *F. flava*/*cerina* clade and *F. masoni* clade. We did not recover a monophyletic *F. cerina* or *F. lananensis*; thus, we collapsed a clade comprising *F. cerina* and *F. flava* and a clade comprising *F. askewi* and *F. lananensis* (Fig. 4). Estimates of the divergence time between two *cox1* substitution rates showed similar values (Table 3). Major diversifications of *Fusconaia* lineages probably occurred during the late Miocene epoch (11.6–5.3 Mya; Fig. 4; Table 3). Median estimates of the split of the Western Gulf/Sabine–Trinity lineages (i.e. *F. askewi*, *F. chunii*, *F. lananensis* and *F. mitchelli*) from the rest of the Mississippian *Fusconaia* species ranged from 9.73 to 7.94 Mya (Fig. 4, node A), followed by the split between the Escambia–Choctawhatchee Province lineage (i.e. *F. burkei* and *F. escambia*) ~9.18–7.52 Mya (Fig. 4, node B; Table 3). The Atlantic *Fusconaia* lineage (i.e. *F. masoni*) split from the Mississippian *Fusconaia* (i.e. *F. cerina* and *F. flava*) ~8.38–7.11 Mya (Fig. 4, node C; Table 3). Finally, the Western Gulf lineage (i.e. *F. mitchelli*) split from the Sabine–Trinity Province lineage (i.e. *F. askewi*, *F. chunii* and *F. lananensis*) ~7.31–5.97 Mya during the late Miocene epoch (Fig. 4, node D; Table 3).

The split between *F. askewi*/*F. lananensis* from the Neches and Sabine rivers and *F. chunii* from the Trinity River was recent, ~2.49–2.03 Mya, during the early Pleistocene epoch (Fig. 4, node E; Table 3). Likewise, *F. burkei* from the Choctawhatchee River and *F. escambia* from the Escambia River were separated ~2.14–1.74 Mya (Fig. 4, node F; Table 3). The 95% credible intervals for these divergence times ranged from the late Pliocene and mid-Pleistocene epochs (Table 3).

Species delimitation analyses based on two GMYC methods yielded similar patterns, which generally agreed with the nominal *Fusconaia* species (Fig. 3). We identified 13 putative species from bGMYC and 18 from ST-GMYC. Both methods recognized *F. chunii* as a putative species, but they also identified multiple putative species within the clade of *F. cerina* and *F. flava* and the clade of *F. askewi* and *F. lananensis* (Fig. 3). Both methods recognized: (1) a clade of *F. cerina* from the Tombigbee River; and (2) a clade composed of *F. cerina* from the Pascagoula River and *F. flava* from the Pearl River as putative species, respectively (Fig. 3). Only the ST-GMYC method identified three putative species within a clade of *F. askewi* and *F. lananensis*.

We analysed shells from 236 individuals for the Fourier morphometric analysis (Supporting Information, Table S2). We assigned these individuals into five groups: *F. askewi* from the Neches River (N = 64), *F. askewi* from the Sabine River (N = 40), *F. chunii* from the Trinity River (N = 41), *F. flava* from

represent maximum likelihood bootstrap support. The tree was rooted with *Arcidens confragosus*. Results of two species delimitation models, the Bayesian generalized mixed Yule-coalescent (bGMYC) and the single-threshold generalized mixed Yule-coalescent ST-GMYC, are shown in vertical bars that correspond to clades in the Bayesian inference phylogeny on the left and represent a putative species from the delimitation methods. Bold bars along clades on the right correspond to the focal species.

Table 1. Summary statistics for *cox1*, *nad1* and ITS1 for *Fusconaia askewi* from the Neches and Sabine rivers, *Fusconaia cerina* from the Gulf of Mexico coastal drainages, *Fusconaia chunii* from the Trinity River, *Fusconaia flava* from the Trinity River (including the San Jacinto River) and elsewhere, and *Fusconaia lananensis* from the Neches River

Species	Drainage	*cox1*				*nad1*				ITS1			
		N	*H*	*K*	π	*N*	*H*	*K*	π	*N*	*H*	*K*	π
Fusconaia askewi	Neches	32	7	1.1	0.0025	24	7	1.8	0.0032	13	1	0	0
Fusconaia askewi	Sabine	62	10	1.0	0.0022	39	12	2.4	0.0047	26	5	0.4	0.0008
Fusconaia cerina	Gulf drainages	6	5	6.6	0.0114	4	2	5.5	0.0091	4	3	4.5	0.0103
Fusconaia chunii	Trinity	44	6	1.3	0.0021	42	5	0.6	0.0012	32	3	0.1	0.0003
Fusconaia flava	Trinity	28	4	0.9	0.0015	28	5	0.7	0.0013	19	2	0.1	0.0006
Fusconaia flava	Widespread	85	26	2.2	0.0064	23	13	4.9	0.0082	11	4	1.3	0.0028
Fusconaia lananensis	Neches	13	4	1.3	0.0024	3	2	0.7	0.0011	–	–	–	–

H, number of haplotypes; *K*, mean number of base pair differences; *N*, number of samples; π, nucleotide diversity.

the Trinity River (N = 29) and widespread *F. flava* (N = 64). The PCA yielded eight distinct eigenvalues and described > 90% of the total variation among individuals (Fig. 5A). The PC1 axis described 42% and the PC2 axis 25% of the total variation. The PCA plot with groups assigned by species showed that morphological variation was similar across all three species, although *F. flava* showed more morphological variation across its geographical distribution (Fig. 5A, B).

The MANOVA revealed that shell morphologies were significantly different between all pairs of groups (Wilk's $\Lambda = 0.1613$; $F_{40,843.7} = 13.03$; $P < 0.001$), except between *F. chunii* and *F. flava* from the Trinity River ($P = 0.736$). On average, the DFA assigned 57% of individuals to the correct group, but correct assignment varied by species and drainage (Table 4). The DFA correctly classified 97% and 76% of individuals from the Neches and Sabine rivers, respectively, as *F. askewi* (Table 4). In contrast, the DFA was less accurate in correctly assigning individuals to *F. chunii* (59%) or *F. flava* from the Trinity River (28%) and unable to differentiate these two species. A total of 48% of *F. flava* from the Trinity River were incorrectly assigned as *F. chunii*. Interestingly, correct classification of *F. flava* from outside the Trinity River was high (69%), and all incorrect classifications were assigned as *F. askewi*.

DISCUSSION

Molecular phylogenetic and species delimitation analyses revealed that *F. chunii* was genetically distinct from *F. askewi*, and *F. lananensis* and *F. cerina* were not genetically distinct from *F. askewi* and *F. flava*, respectively. Our results provide clarification that *F. askewi* and *F. chunii* represent two distinct evolutionary lineages, as each formed a reciprocally monophyletic lineage (Fig. 3). Genetic divergence between the taxa was relatively small compared with other closely related mussel species (Roe & Lydeard, 1998; Inoue *et al.*, 2013), but greater than those between *Arcidens confragosus* and *Arcidens wheeleri* (Ortmann & Walker, 1912) (Inoue *et al.*, 2014a) and between *F. burkei* and *F. escambia* (Pfeiffer *et al.*, 2016). Shell morphologies between *F. askewi* and *F. chunii* were statistically distinct. Within *F. askewi*, there was no geographical structure between populations, and several haplotypes were shared between the Neches and Sabine populations, suggesting current or recent gene flow between the drainages. Furthermore, genetic differentiation between *F. chunii* and *F. askewi* would be expected given that the Trinity River is separated from the Neches and Sabine rivers by the Gulf of Mexico. Based on the reciprocal monophyly and allopatric distributions, it is likely that *F. askewi* and *F. chunii* have undergone recent speciation. Our molecular clock analyses support this inference, as divergence is estimated to have occurred in the mid-Pleistocene epoch (Fig. 4). Therefore, we recognize *F. chunii* as a distinct species and conclude that there are three *Fusconaia* species in the Sabine–Trinity Province (*F. askewi*, *F. chunii* and *F. flava*) and that *F. lananensis* is a junior synonym of *F. askewi*. Likewise, *F. cerina* is likely to be a junior synonym of *F. flava* based on the fact that *F. cerina* was genetically indistinguishable from *F. flava*.

In addition to *F. chunii*, the Trinity River has syntopic *F. flava* whose morphologies are indistinguishable from those of *F. chunii*. Previously, the distribution of *F. flava* in the Sabine–Trinity Province was unclear owing to the inability to distinguish them morphologically from *F. askewi* or *F. chunii* (Howells *et al.*, 1996). Hydrology, local environmental conditions, and stream position are known to cause ecophenotypic variation in mussels (Ortmann, 1920; Inoue *et al.*, 2013). In the case of *F. flava*, their wide geographical distribution

Table 2. Mean pairwise genetic divergences for the concatenated mitochondrial DNA (below diagonal) and ITS1 (above diagonal) sequences from *Fusconaia askewi* (Neches and Sabine rivers), *F. cerina*, *F. chunii*, *F. flava* (Trinity River and elsewhere) and *F. lananensis*

	Fusconaia askewi (Neches)	*Fusconaia askewi* (Sabine)	*Fusconaia cerina* (Gulf drainage)	*Fusconaia chunii* (Trinity)	*Fusconaia flava* (Trinity)	*Fusconaia flava* (widespread)	*Fusconaia lananensis* (Neches)
Fusconaia askewi (Neches)		0.0007	0.0049	0.0001	0.0002	0.0016	–
Fusconaia askewi (Sabine)	0.0034		0.0054	0.0008	0.0009	0.0022	–
Fusconaia cerina (Gulf drainage)	0.0375	0.0375		0.0050	0.0051	0.0061	–
Fusconaia chunii (Trinity)	0.0096	0.0098	0.0379		0.0003	0.0017	–
Fusconaia flava (Trinity)	0.0361	0.0363	0.0105	0.0371		0.0018	–
Fusconaia flava (widespread)	0.0366	0.0365	0.0117	0.0386	0.0057		–
Fusconaia lananensis (Neches)	0.0026	0.0033	0.0391	0.0123	0.0380	0.0367	

has probably shaped the morphological variation observed within this species, which presumably is in response to local environmental conditions (Graf, 1998). In fact, our morphometric results reveal high morphological plasticity within *F. flava* (Fig. 5). These results support the assertion that molecular methods are often necessary when distinguishing between some freshwater mussel species (Shea *et al.*, 2011) and necessary to separate *F. flava* from *F. chunii* in the Trinity River. Possible explanations for the lack of genetic structure and low genetic divergence among drainages for *F. flava* is that it has high dispersal capability via the movement of fish hosts, which may have allowed rapid range expansion to formerly glaciated areas (Elderkin *et al.*, 2007; Inoue *et al.*, 2014b). Consequently, populations of *F. flava* in the Trinity River (including the San Jacinto River) were probably derived from recent dispersal into the basin. However, we cannot rule out anthropogenic relocation of *F. flava* to the Trinity River, because other freshwater mussel species have reportedly been moved into the drainage to improve the quality of commercial shell resources.

Forces driving speciation of Gulf Coast *Fusconaia*

Major diversification within the genus *Fusconaia* occurred during the mid-Miocene to Pliocene epochs, when the Western Gulf and Sabine–Trinity Province lineages were separated from the rest of Mississippian Region lineages (Fig. 4, node A). The timing of the diversification is congruent with patterns of fish endemism in the region (Conner & Suttkus, 1986; Hoagstrom *et al.*, 2013; Osborne *et al.*, 2016). During the late Neogene period (late Miocene to Pliocene), mountain uplifts and strong east-to-west climatic gradients created high erosion rates of alluvial plains, which formed three ancestral 'mega-drainages' in the Gulf coastal plain (Galloway *et al.*, 2011; Hoagstrom *et al.*, 2013). This caused the Mega-Mississippi River to become the largest drainage entering the Gulf of Mexico (Blum & Aslan, 2006). During the late Miocene, the ancestral Guadalupe River separated from the Mega-Brazos River (currently the Brazos, Calcasieu, Neches, Sabine and Trinity rivers) as a result of increasing aridity during this epoch (Galloway *et al.*, 2011; Osborne *et al.*, 2016). These changes resulted in the elimination of some freshwater habitats, which has been hypothesized as the cause of extirpation of ancestral *Cyprinella lutrensis* (Baird & Girard, 1853) from the ancestral Guadalupe River and Rio Grande basins during the Miocene (Galloway *et al.*, 2011; Osborne *et al.*, 2016). Likewise, the separation of the ancestral Guadalupe and Mega-Brazos rivers probably caused a reduction in the range of ancestral

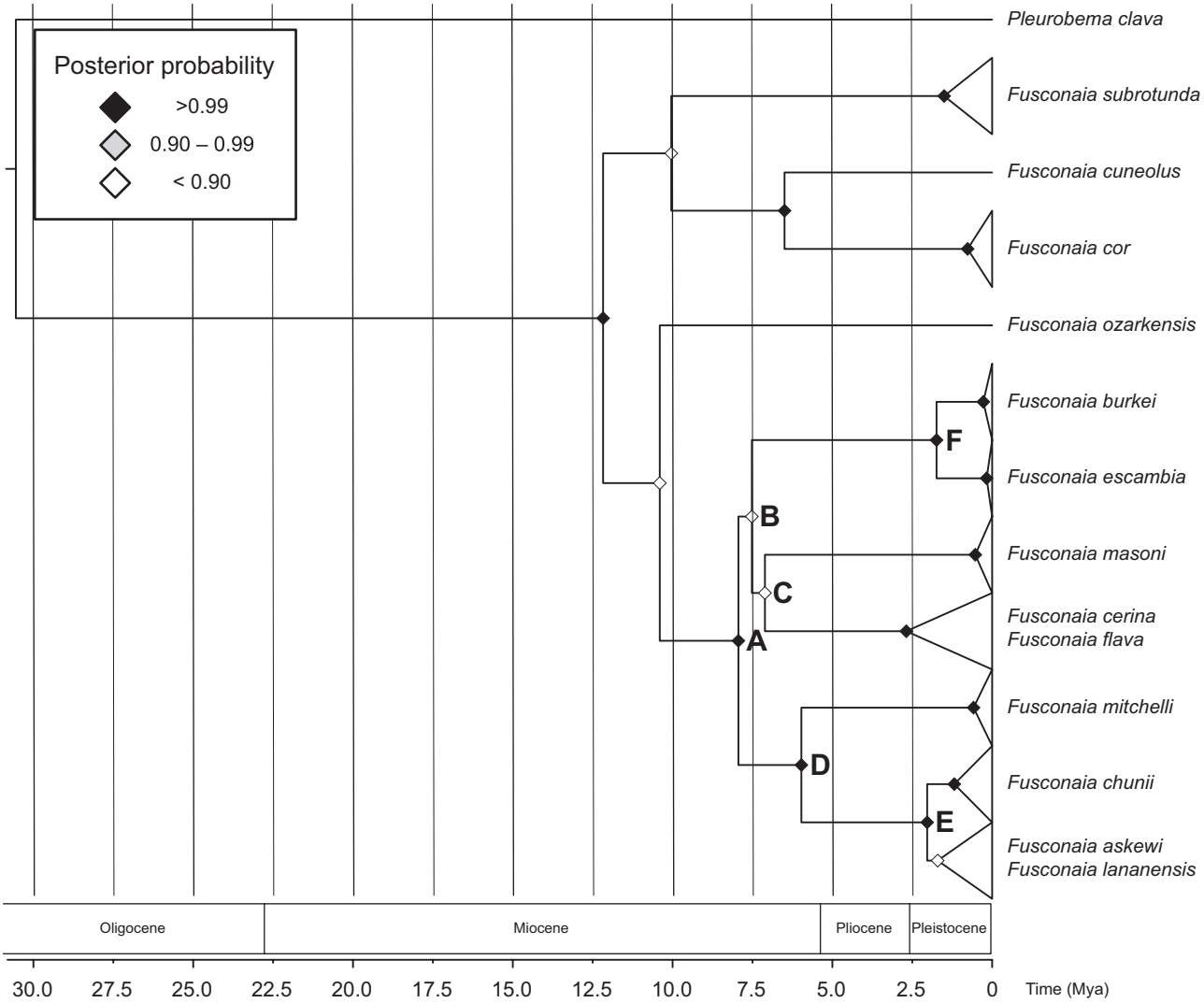

Figure 4. Maximum clade credible tree based on the mitochondrial DNA + nuclear DNA dataset analysed from BEAST. Nodes A–F are specific divergence points (see Table 3). Divergence time is scaled to million years ago. Bayesian posterior probabilities are shown in shaded diamonds along the nodes (white < 0.91, grey = 0.91–0.99, black > 0.99).

Table 3. Divergence-time (million years ago) estimates for the most recent common ancestor of *Fusconaia* species

Node	Divergence events	Bolotov *et al.* (2016)	Froufe *et al.* (2016)
A	Split of the Western Gulf/Sabine–Trinity Province lineages from the rest of the Atlantic/Mississippian lineages	9.73 (7.20–12.32)	7.94 (5.95–10.14)
B	Split of the Escambia–Choctawhatchee Province lineages from Atlantic/Mississippian lineages	9.18 (6.30–11.13)	7.52 (5.16–9.23)
C	Split of the Atlantic lineage from the Mississippian lineage	8.38 (5.04–10.15)	7.11 (4.39–8.25)
D	Split of the Western Gulf and Sabine–Trinity Province lineages	7.31 (5.16–9.61)	5.97 (4.19–7.84)
E	Split of *Fusconaia askewi* and *Fusconaia chunii*	2.49 (1.59–3.47)	2.03 (1.28–2.83)
F	Split of *Fusconaia burkei* and *Fusconaia escambia*	2.14 (0.93–3.54)	1.74 (0.74–2.85)

Node labels correspond to Fig. 4. Divergence times were estimated in BEAST with a relaxed lognormal molecular clock and Yule model. Two *cox1* substitution rates were used: 1.68×10^{-9} to 2.86×10^{-9} substitutions per site year^{-1} (Bolotov *et al.*, 2016) and $2.56 \times 10^{-9} \pm 0.6 \times 10^{-9}$ substitutions per site year^{-1} (Froufe *et al.*, 2016). Values are the median divergence time (million years ago) with 95% credible interval in parentheses. Names of regions and provinces are based on Neck (1982) and Haag (2010).

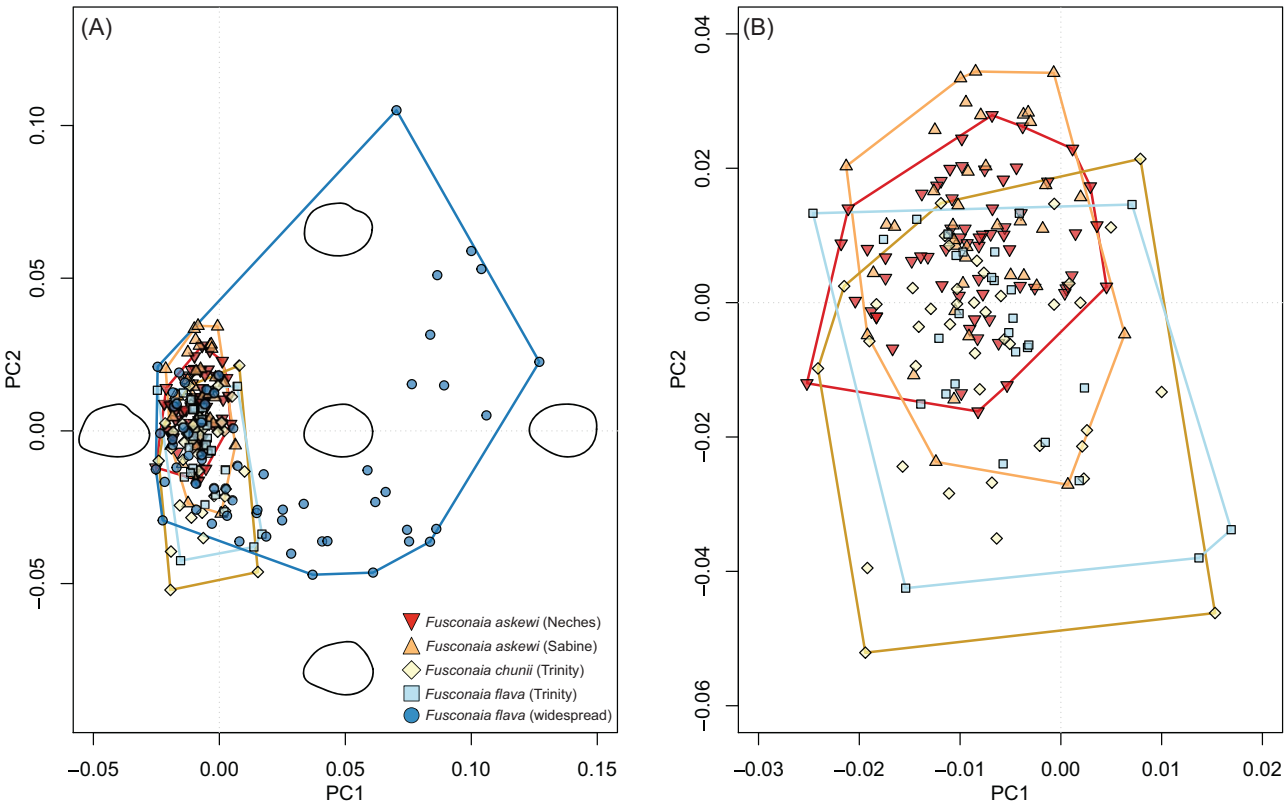

Figure 5. Biplots from principal component analysis (PCA) of Fourier morphometrics for all individuals (A) and all except widespread *Fusconaia flava* (B). Colours and shapes of points correspond to species and collected drainages (red upright triangles, *Fusconaia askewi* from the Neches River; orange upside-down triangles, *F. askewi* from the Sabine River; yellow diamonds, *Fusconaia chunii* from the Trinity River; light blue squares, *F. flava* from the Trinity River; dark blue circles, widespread *F. flava*). Polygons enclose convex hulls of each group. Outlined shell shapes represent a mean shape (meddle) and ±2 × SD on PC1 and PC2 axes.

Fusconaia lineages, which later split into *F. mitchelli* and the most recent common ancestor of *F. askewi* and *F. chunii* (Fig. 4, node D), followed by separation of *F. askewi* in the Neches and Sabine rivers and *F. chunii* in the Trinity River (Fig. 4, node E).

The modern fluvial systems of North America began to form in the Pliocene–Pleistocene epochs owing to global climate change (Galloway *et al.*, 2011). Runoff from the glaciation events entrenched the current Mississippi River system and redeveloped the western Gulf coastal drainages (Galloway *et al.*, 2011). During the Pleistocene epoch, rivers in the Sabine–Trinity Province received high discharge and created new channels (Tockner *et al.*, 2010; Galloway *et al.*, 2011). During the same period, the Neches River temporarily became a tributary of the Sabine River (Phillips, 2008), which probably explains the absence of phylogeographical structuring and sharing of haplotypes between the Neches and Sabine populations of *F. askewi*. Although estuary zones of the Sabine and Trinity rivers were connected during the late Pleistocene, the ancestral Trinity River was separated from other larger river basins via barriers that were created by the accumulation of sediment deposits during sea-level change (Blum & Aslan, 2006). This separation probably caused allopatric diversification of *F. chunii* in the Trinity River. Likewise, phylogeographical analyses of amplified fragment length polymorphism (AFLP) genotypes of the topminnow *Fundulus notatus* (Rafinesque, 1820) showed separation between the Trinity and Neches/Sabine clades (Duvernell *et al.*, 2013).

The lack of phylogeographical pattern indicates that the current distribution of *F. flava*, which includes the entire Mississippi River basin, Great Lakes systems, Mobile River basin and east and west Gulf coastal drainages, is probably the result of range expansion during the late Pleistocene to Holocene. Specifically, stream capture between the current tributaries of the Mississippi River coupled with sea-level fluctuations that joined currently unconnected systems is thought to have allowed aquatic species to disperse throughout Gulf coastal rivers (Roe, Hartfield & Lydeard, 2001; Burdick & White, 2007). Such rapid expansion of

Table 4. Confusion matrix with proportions of individuals in a priori species classification (rows) that are assigned to the predicted species (columns) based on a discriminant function analysis

	Fusconaia askewi (Neches)	*Fusconaia askewi* (Sabine)	*Fusconaia chunii* (Trinity)	*Fusconaia flava* (Trinity)	*Fusconaia flava* (widespread)
Fusconaia askewi (Neches)	0.78	0.19	0	0.02	0.02
Fusconaia askewi (Sabine)	0.23	0.53	0.05	0.18	0.03
Fusconaia chunii (Trinity)	0.05	0.07	0.59	0.29	0
Fusconaia flava (Trinity)	0.07	0.10	0.48	0.28	0.07
Fusconaia flava (widespread)	0.27	0.03	0	0	0.69

A priori species classification includes *F. askewi* from the Neches and Sabine rivers, *F. chunii* from the Trinity River, and *F. flava* from the Trinity River (including the San Jacinto River) and elsewhere. Diagonal values indicate a proportion of individuals in a priori species classification that are correctly predicted to the species.

species range has been inferred on the basis of genetic evidence in other widely distributed mussel species (Elderkin *et al.*, 2008; Inoue *et al.*, 2014a, b).

Discriminating power of ITS1 and morphometric markers

We observed low genetic variability of ITS1 sequences, where four nominal species (*F. askewi*, *F. cerina*, *F. chunii* and *F. flava*) shared a single haplotype of ITS1 (Fig. 2; Supporting Information, Fig. S2). Low genetic variability at ITS1 is a common issue among phylogenetic studies of freshwater mussels (Serb, 2006; Campbell & Lydeard, 2012a, b), which raises the question of the utility of ITS1 for molecular systematic analyses. Multi-locus genetic markers with phylogenetically meaningful resolution, such as restriction-associated DNA sequences (RADseq), might provide a better approach.

In our morphometric analyses, using Fourier morphometrics we were able to differentiate the current nominal species statistically, except for *F. chunii* from *F. flava* from the Trinity River, which is probably because this analysis compares differences in shell outline only. Incorporating three-dimensional models that can capture variation of shell height and width might prove more useful for identifying characters that enable correct identification of the respective species.

Implication for conservation

Understanding the evolutionary modes of speciation and genetic diversity of declining populations can provide information to identify cryptic species and guide efforts focused on ensuring long-term persistence of imperiled fauna. Regions with high levels of endemism often experience strong selective pressures owing to restricted available habitat or geographical range, which can lead to disproportionate rates of extirpation or extinction for endemic species when combined with anthropogenic perturbations (Malcolm *et al.*, 2006; Burkhead, 2012). Thus, in areas where high levels of endemism are known or suspected to occur, conservationists could focus efforts initially on refining knowledge of the systematics, taxonomy and genetic structure of common and rare species to ensure protection of cryptic diversity and future adaptive capacity. These data, in conjunction with distribution information, provide a sound foundation for future mitigation and recovery activities.

Based on our findings, the distribution of *F. askewi* probably includes only the Neches and Sabine rivers, which represents a reduction in presumptive range for this species. Currently, *F. askewi* is listed as threatened by the State of Texas (TPWD, 2010) and has yet to be considered for ESA listing by the USFWS. Currently, *F. lananensis* is listed as threatened by Texas and has been proposed by USFWS for listing under the ESA (USFWS, 2009); however, our findings show that this species is a junior synonym of *F. askewi*, and its proposed listing by USFWS may not be warranted. Our results suggest that *F. chunii* is a valid species and, based on recent surveys in this drainage, it appears to have a restricted distribution, occurring in the mainstem of the Trinity River near Dallas-Fort Worth to just above Lake Livingston and adjacent tributaries (e.g. the Clear, East, Elm and West forks; Randklev *et al.*, 2017). Owing to the restricted distribution of this species, mostly downstream of a highly urbanized landscape, it might be a candidate for listing at the state and federal levels.

Our results provide a case study on the importance of integrating taxonomy, phylogeny and population genetics into conservation planning and echo the call by other conservationists working with freshwater mussels for further research on these topics (NNMCC, 1998; Haag & Williams, 2014; FMCS, 2016). Particularly in places like Texas, where freshwater mussel conservation is in its infancy, a holistic approach such as used in this study can provide information needed to make critical decisions in freshwater mussel management.

ACKNOWLEDGEMENTS

Field and laboratory assistance was provided by the Texas Parks and Wildlife Department, Tony Brady, Chris Eads, Jeff Garner, Paul Hartfield, David Hayes, Bob Jones, Bill Posey, Sandy Pursifull, Josh Seagraves, Todd Slack, Jim Williams and Randklev laboratory members. Funding was provided by the Texas Parks and Wildlife Department and the US Fish and Wildlife Service. We thank Eric Hallerman, the editor, and two anonymous referees for helpful comments on earlier draft of this manuscript. The authors declare no conflict of interest. Any use of trade, firm or product names is for descriptive purposes only and does not imply endorsement by the United States Government.

REFERENCES

Berendzen PB, Simons AM, Wood RM, Dowling TE, Secor CL. 2007. Recovering cryptic diversity and ancient drainage patterns in eastern North America: historical biogeography of the *Notropis rubellus* species group (Teleostei: Cypriniformes). *Molecular Phylogenetics and Evolution* **46:** 721–737.

Blum MD, Aslan A. 2006. Signatures of climate vs. sea-level change within incised valley-fill successions: quaternary examples from the Texas Gulf Coast. *Sedimentary Geology* **190:** 177–211.

Bogan AE, Roe KJ. 2008. Freshwater bivalve (Unioniformes) diversity, systematics, and evolution: status and future directions. *Journal of the North American Benthological Society* **27:** 349–369.

Bolotov IN, Vikhrev IV, Bespalaya YV, Gofarov MY, Kondakov AV, Konopleva ES, Bolotov NN, Lyubas AA. 2016. Multi-locus fossil-calibrated phylogeny, biogeography and a subgeneric revision of the Margaritiferidae (Mollusca: Bivalvia: Unionoida). *Molecular Phylogenetics and Evolution* **103:** 104–121.

Bouckaert R, Heled J, Kühnert D, Vaughan T, Wu CH, Xie D, Suchard MA, Rambaut A, Drummond AJ. 2014. BEAST 2: a software platform for Bayesian evolutionary analysis. *PLoS Computational Biology* **10:** e1003537.

Burdick RC, White MM. 2007. Phylogeography of the Wabash Pigtoe, *Fusconaia flava* (Rafinesque, 1820) (Bivalvia: Unionidae). *Journal of Molluscan Studies* **73:** 367–375.

Burkhead NM. 2012. Extinction rates in North American freshwater fishes, 1900–2010. *Bioscience* **62:** 798–808.

Burlakova LE, Campbell D, Karatayev AY, Barclay D. 2012. Distribution, genetic analysis and conservation priorities for rare Texas freshwater molluscs in the genera *Fusconaia* and *Pleurobema* (Bivalvia: Unionidae). *Aquatic Biosystems* **8:** 12.

Burr BM, Mayden RL. 1992. Phylogenetics and North American freshwater fishes. In: Mayden RL, ed. *Systematics, historical ecology, and North American freshwater fishes*. Stanford, CA: Stanford University Press, 18–75.

Campbell DC, Lydeard C. 2012a. Molecular systematics of *Fusconaia* (Bivalvia: Unionidae: Ambleminae). *American Malacological Bulletin* **30:** 1–17.

Campbell DC, Lydeard C. 2012b. The genera of Pleurobemini (Bivalvia: Unionidae: Ambleminae). *American Malacological Bulletin* **30:** 19–38.

Campbell DC, Serb JM, Buhay JE, Roe KJ, Minton RL, Lydeard C. 2005. Phylogeny of North American amblemines (Bivalvia: Unionoida): prodigious polyphyly proves pervasive across genera. *Invertebrate Biology* **124:** 131–164.

Clement M, Posada D, Crandall KA. 2000. TCS: a computer program to estimate gene genealogies. *Molecular Ecology* **9:** 1657–1659.

Conner JV, Suttkus RD. 1986. Zoogeography of freshwater fishes of the Western Gulf slope. In: Hocutt CH, Wiley EO, eds. *Zoogeography of North American freshwater fishes*. New York, NY: John Wiley & Sons, Inc.

Conrad TA. 1838. Monography of the Family Unionidae, or naiades of Lamarck (fresh water bivalve shells) or North America, illustrated by figures drawn on stone from nature. Philadelphia, PA: J. Dobson. **11:** 95–102.

Duvernell DD, Meier SL, Schaefer JF, Kreiser BR. 2013. Contrasting phylogeographic histories between broadly sympatric topminnows in the *Fundulus notatus* species complex. *Molecular Phylogenetics and Evolution* **69:** 653–663.

Elderkin CL, Christian AD, Metcalfe-Smith JL, Berg DJ. 2008. Population genetics and phylogeography of freshwater mussels in North America, *Elliptio dilatata* and *Actinonaias ligamentina* (Bivalvia: Unionidae). *Molecular Ecology* **17:** 2149–2163.

Elderkin CL, Christian AD, Vaughn CC, Metcalfe-Smith JL, Berg DJ. 2007. Population genetics of the freshwater mussel, *Amblema plicata* (Say 1817) (Bivalvia: Unionidae): evidence of high dispersal and post-glacial colonization. *Conservation Genetics* **8:** 355–372.

Ezard T, Fujisawa T, Barraclough T. 2013. *R package splits: SPecies' LImits by Threshold Statistics, version 1.0*. Available at: https://r-forge.r-project.org/projects/splits/

FMCS (Freshwater Mollusk Conservation Society). 2016. A national strategy for the conservation of native freshwater mollusks. *Freshwater Mollusk Biology and Conservation* **19:** 1–21.

Folmer O, Black M, Hoeh W, Lutz R, Vrijenhoek R. 1994. DNA primers for amplification of mitochondrial cytochrome *c* oxidase subunit I from diverse metazoan invertebrates. *Molecular Marine Biology and Biotechnology* **3:** 294–299.

Froufe E, Gonçalves DV, Teixeira A, Sousa R, Varandas S, Ghamizi M, Zieritz A, Lopes-Lima M. 2016. Who lives where? Molecular and morphometric analyses clarify which *Unio* species (Unionida, Mollusca) inhabit the southwestern Palearctic. *Organisms Diversity & Evolution* **16:** 597–611.

Fujita MK, Leaché AD, Burbrink FT, McGuire JA, Moritz C. 2012. Coalescent-based species delimitation in an integrative taxonomy. *Trends in Ecology & Evolution* **27:** 480–488.

Galloway WE, Whiteaker TL, Ganey-Curry P. 2011. History of Cenozoic North American drainage basin evolution, sediment yield, and accumulation in the Gulf of Mexico basin. *Geosphere* **7:** 938–973.

Graf DL. 1998. Freshwater pearly mussels: pigtoes and Ortmann's Law. *American Conchologist* **26:** 20–21.

Graf DL. 2013. Patterns of freshwater bivalve global diversity and the state of phylogenetic studies on the Unionoida, Sphaeriidae, and Cyrenidae. *American Malacological Bulletin* **31:** 135–153.

Graf DL, Cummings KS. 2007. Review of the systematics and global diversity of freshwater mussel species (Bivalvia: Unionoida). *Journal of Molluscan Studies* **73:** 291–314.

Haag WR. 2010. A hierarchical classification of freshwater mussel diversity in North America. *Journal of Biogeography* **37:** 12–26.

Haag WR. 2012. *North American freshwater mussels: natural history, ecology, and conservation*. Cambridge, UK: Cambridge University Press.

Haag WR, Williams JD. 2014. Biodiversity on the brink: an assessment of conservation strategies for North American freshwater mussels. *Hydrobiologia* **735:** 45–60.

Helaers R, Milinkovitch MC. 2010. MetaPIGA v2.0: maximum likelihood large phylogeny estimation using the metapopulation genetic algorithm and other stochastic heuristics. *BMC Bioinformatics* **11:** 379.

Hoagstrom CW, Ung V, Taylor K, Ebach M. 2013. Miocene rivers and taxon cycles clarify the comparative biogeography of North American highland fishes. *Journal of Biogeography* **41:** 644–658.

Howells RG. 2010. *Freshwater mussels of Texas and the western Gulf Coast. Freshwater Mollusk Conservation Society 2010 workshop: regional fauna identification and sampling*. Kirkwood, MO, 161–174.

Howells RG, Neck RW, Murray HD. 1996. *Freshwater mussels of Texas*. Austin, TX: Texas Park and Wildlife Department.

Inoue K, Hayes DM, Harris JL, Christian AD. 2013. Phylogenetic and morphometric analyses reveal ecophenotypic plasticity in freshwater mussels *Obovaria jacksoniana* and *Villosa arkansasensis* (Bivalvia: Unionidae). *Ecology and Evolution* **3:** 2670–2683.

Inoue K, Hayes DM, Harris JL, Johnson NA, Morrison CL, Eackles MS, King TL, Jones JW, Hallerman EM, Christian AD, Randklev CR. 2018. The Pleurobemini (Bivalvia: Unionida) revisited: molecular species delineation using a mitochondrial DNA gene reveals multiple conspecifics and undescribed species. *Invertebrate Systematics*. Doi:10.1071/IS17059.

Inoue K, Lang BK, Berg DJ. 2015. Past climate change drives current genetic structure of an endangered freshwater mussel species. *Molecular Ecology* **24:** 1910–1926.

Inoue K, McQueen AL, Harris JL, Berg DJ. 2014a. Molecular phylogenetics and morphological variation reveal recent speciation in freshwater mussels of the genera *Arcidens* and *Arkansia* (Bivalvia: Unionidae). *Biological Journal of the Linnean Society* **112:** 535–545.

Inoue K, Monroe EM, Elderkin CL, Berg DJ. 2014b. Phylogeographic and population genetic analyses reveal Pleistocene isolation followed by high gene flow in a wide ranging, but endangered, freshwater mussel. *Heredity* **112:** 282–290.

Iwata H, Ukai Y. 2002. SHAPE: a computer program package for quantitative evaluation of biological shapes based on elliptic Fourier descriptors. *Journal of Heredity* **93:** 384–385.

Katoh K, Standley DM. 2013. MAFFT multiple sequence alignment software version 7: improvements in performance and usability. *Molecular Biology and Evolution* **30:** 772–780.

King TL, Eackles MS, Gjetvaj B, Hoeh WR. 1999. Intraspecific phylogeography of *Lasmigona subviridis* (Bivalvia: Unionidae): conservation implications of range discontinuity. *Molecular Ecology* **8:** S65–S78.

Kumar S, Stecher G, Tamura K. 2016. MEGA7: Molecular Evolutionary Genetics Analysis version 7.0 for bigger datasets. *Molecular Biology and Evolution* **33:** 1870–1874.

Librado P, Rozas J. 2009. DnaSP v5: a software for comprehensive analysis of DNA polymorphism data. *Bioinformatics* **25:** 1451–1452.

Malcolm JR, Liu C, Neilson RP, Hansen L, Hannah L. 2006. Global warming and extinctions of endemic species from biodiversity hotspots. *Conservation Biology* **20:** 538–548.

Mayden RL. 1988. Vicariance biogeography, parsimony, and evolution in North American freshwater fishes. *Systematic Zoology* **37:** 329–355.

Mayden RL. 1992. *Systematics, historical ecology, and North American freshwater fishes*. Stanford, CA: Stanford University Press.

Near TJ, Benard MF. 2004. Rapid allopatric speciation in logperch darters (Percidae: *Percina*). *Evolution* **58:** 2798–2808.

Neck RW. 1982. Preliminary analysis of the ecological zoogeography of the freshwater mussels of Texas. In: Davis JR, ed. Proceedings of the symposium on recent benthological investigations in Texas and adjacent states. Austin, TX: Texas Academy of Science, 33–42.

NNMCC (National Native Mussel Conservation Committee). 1998. National strategy for the conservation of native freshwater mussels. *Journal of Shellfish Research* **17:** 1419–1428.

Ortmann AE. 1920. Correlation of shape and station in fresh-water mussels (Naiades). *Proceedings of the American Philosophical Society* **59:** 268–312.

Osborne MJ, Diver TA, Hoagstrom CW, Turner TF. 2016. Biogeography of '*Cyprinella lutrensis*': intensive genetic sampling from the Pecos River 'melting pot' reveals a dynamic history and phylogenetic complexity. *Biological Journal of the Linnean Society* **117:** 264–284.

Pfeiffer JM, III, Johnson NA, Randklev CR, Howells RG, Williams JD. 2016. Generic reclassification and species boundaries in the rediscovered freshwater mussel '*Quadrula*' *mitchelli* (Simpson in Dall, 1896). *Conservation Genetics* **17:** 279–292.

Phillips JD. 2008. Geomorphic controls and transition zones in the lower Sabine River. *Hydrological Processes* **22:** 2424–2437.

Pons J, Barraclough TG, Gomez-Zurita J, Cardoso A, Duran DP, Hazell S, Kamoun S, Sumlin WD, Vogler AP. 2006. Sequence-based species delimitation for the DNA taxonomy of undescribed insects. *Systematic Biology* **55:** 595–609.

Rambaut A, Drummond AJ. 2009. *Tracer v1.5*. Available at: http://tree.bio.ed.ac.uk/software/tracer/

Randklev CR, Inoue K, Hart M, Pieri A. 2017. *Assessing the conservation status of native freshwater mussels (Family: Unionidae) in the Trinity River basin; final report*. College Station, TX: Texas A&M Institute of Renewable Natural Resources, 55.

Reid NM, Carstens BC. 2012. Phylogenetic estimation error can decrease the accuracy of species delimitation: a Bayesian implementation of the general mixed Yule-coalescent model. *BMC Evolutionary Biology* **12:** 196.

Roe KJ, Hartfield PD, Lydeard C. 2001. Phylogeographic analysis of the threatened and endangered superconglutinate-producing mussels of the genus *Lampsilis* (Bivalvia: Unionidae). *Molecular Ecology* **10:** 2225–2234.

Roe KJ, Lydeard C. 1998. Molecular systematics of the freshwater mussel genus *Potamilus* (Bivalvia: Unionidae). *Malacologia* **39:** 195–206.

Ronquist F, Teslenko M, van der Mark P, Ayres DL, Darling A, Höhna S, Larget B, Liu L, Suchard MA, Huelsenbeck JP. 2012. MrBayes 3.2: efficient Bayesian phylogenetic inference and model choice across a large model space. *Systematic Biology* **61:** 539–542.

Saghai-Maroof MA, Soliman KM, Jorgensen RA, Allard RW. 1984. Ribosomal DNA spacer-length polymorphisms in barley: Mendelian inheritance, chromosomal location, and population dynamics. *Proceedings of the National Academy of Sciences of the United States of America* **81:** 8014–8018.

Serb JM. 2006. Discovery of genetically distinct sympatric lineages in the freshwater mussel *Cyprogenia aberti* (Bivalvia: Unionidae). *Journal of Molluscan Studies* **72:** 425–434.

Shea CP, Peterson JT, Wisniewski JM, Johnson NA. 2011. Misidentification of freshwater mussel species (Bivalvia: Unionidae): contributing factors, management implications, and potential solutions. *Journal of the North American Benthological Society* **30:** 446–458.

Stamatakis A. 2014. RAxML version 8: a tool for phylogenetic analysis and post-analysis of large phylogenies. *Bioinformatics* **30:** 1312–1313.

Strange RM, Burr BM. 1997. Intraspecific phylogeography of North American highland fishes: a test of the Pleistocene vicariance hypothesis. *Evolution* **51:** 885–897.

Tanabe AS. 2011. Kakusan4 and Aminosan: two programs for comparing nonpartitioned, proportional and separate models for combined molecular phylogenetic analyses of multilocus sequence data. *Molecular Ecology Resources* **11:** 914–921.

Thesing BD, Noyes RD, Starkey DE, Shepard DB. 2016. Pleistocene climatic fluctuations explain the disjunct distribution and complex phylogeographic structure of the Southern Red-backed Salamander, *Plethodon serratus*. *Evolutionary Ecology* **30:** 89–104.

Tockner K, Lorang MS, Stanford JA. 2010. River flood plains are model ecosystems to test general hydrogeomorphic and ecological concepts. *River Research and Applications* **26:** 76–86.

TPWD (Texas Parks and Wildlife Department). 2010. Threatened and endangered nongame species. Chapter 65. Wildlife Subchapter G. 31 TAC §65.175. Adopted rules. *Texas Register* **35:** 249–251.

USFWS (US Fish and Wildlife Service). 2009. Endangered and threatened wildlife and plants; partial 90-day finding on a petition to list 475 species in the southwestern United States as threatened or endangered with critical habitat; proposed rule. *Federal Register* **74:** 66866–66905.

Vidrine MF. 1993. *The historical distributions of freshwater mussels in Louisiana*. Eunice, LA: Gail Q. Vidrine Collectibles.

Watters GT, Hoggarth MA, Stansbery DH. 2009. *The freshwater mussels of Ohio*. Columbus, OH: Ohio State University.

Williams JD, Bogan AE, Butler RS, Cummings KS, Garner JT, Harris JL, Johnson NA, Watters GT. 2017. A revised list of the freshwater mussels (Mollusca: Bivalvia: Unionida) of the United States and Canada. *Freshwater Mollusk Biology and Conservation* **20:** 33–58.

SUPPORTING INFORMATION

Additional Supporting Information may be found in the online version of this article at the publisher's web-site:

Table S1. List of specimen information [species, DNA ID, collected waterbody, state, source and GenBank accession numbers for cytochrome *c* oxidase I (*cox1*), NADH dehydrogenase I (*nad1*) and internal transcribed spacer 1 (ITS1)] used in the study. 'Hetero' in the ITS1 column indicates a heterozygous individual. ASUMZ, Arkansas State University Museum of Zoology; FLMNH, Florida Museum of Natural History; GenBank, sequences from GenBank; JBFMC, Texas A&M Natural Resources Institute Freshwater Mussel Collection; MO, Baylor University Mayborn Museum Collection; tissue clip and swab sample, specimen mantle tissue was clipped or swabbed in the field and returned to its source waterbody.

Table S2. List of specimen information [species, source, number of individuals (n), collected waterbody, drainage and state] used for Fourier morphometric analysis in the study. ASUMZ, Arkansas State University Museum of Zoology; JBFMC, Texas A&M Natural Resources Institute Freshwater Mussel Collection.

Figure S1. Phylogenetic tree reconstructed by Bayesian analysis for concatenated mitochondrial DNA (i.e. *cox1* and *nad1*) dataset. Values above branches represent Bayesian posterior probabilities and values below represent maximum likelihood bootstrap support. The tree was rooted with *Arcidens confragosus*. Bold bars along clades correspond to the focal species.

Figure S2. Phylogenetic tree reconstructed by Bayesian analysis for ITS1 dataset. Values above branches represent Bayesian posterior probabilities and values below represent maximum likelihood bootstrap support. The tree was rooted with *Arcidens confragosus*. Bold bars along clades correspond to the focal species.